

# ELECTROMECHANICAL ACTUATOR CASE STUDY: MULTIVARIABLE ANALYSIS OF PHASE CURRENTS TO DETECT THREE TYPES OF FAULTS

James P. Hofmeister, Robert S. Wagoner, Douglas L. Goodman  
Ridgetop Group, Inc.  
3580 West Ina Road  
Tucson, AZ 85741  
520-742-3300

[jhofmeister@ridgetopgroup.com](mailto:jhofmeister@ridgetopgroup.com)

**Abstract:** This paper describes a multiple-variable analysis (MVA) methodology to detect and prognose three types of faults associated with an electromechanical actuator (EMA): (1) loading faults, such as friction, on the shaft of an EMA motor, (2) shorting faults in the stator windings of the EMA motor, and (3) on-resistance faults in one or more power-switching transistors used to convert direct voltage/current into alternating current. The presented methodology overcomes difficulties associated with typical multivariate analysis (as opposed to multiple-variable analysis) methods such as the following examples: solving simultaneous equations and performing a statistical-based analysis such as K-nearest neighbor (KNN) regression and other Euclidean-based distance methods. Examples of those difficulties are the following: (1) analysis methods that produced information suitable for classification rather than diagnosis or prognosis; (2) noisy data; (3) dependent data, rather than independent data; and (4) difficulty in processing test data to identify, extract, and use leading indicators of failure for prognostic purposes. The primary MVA solution methods included (1) noise mitigation, (2) a unique root-mean-square (RMS) of quantifying phase current values, and (3) a combination of nearest neighbor and distance methods of processing phase-current data to unequivocally identify and isolate faults and to prognose a future time at which functional failure is likely to occur.

\*ARULEAV is a trademark of Ridgetop Group, Inc.

**Key words:** Diagnostics; electromechanical actuator; EMA; IVHM; multiple-variable analysis; MVA; prognostics; PHM

## 1. INTRODUCTION

A NASA-funded Small Business Innovation Research (SBIR) program on electromechanical actuators (EMAs) had the following objectives: deliver a Model-based Avionic Prognostic Reasoner (MAPR) for non-intrusive monitoring of the state of health (SoH) and remaining useful life (RUL) of electromechanical assets by using data obtained from a standard avionic data bus: see Figure 1. The following specific faults were identified: (1) loading faults, such as friction, on the shaft of an EMA motor, (2) shorting faults in the stator windings of the EMA motor, and (3) on-resistance faults in one or more power-switching transistors used to convert direct voltage/current into alternating current. [1]-[5]

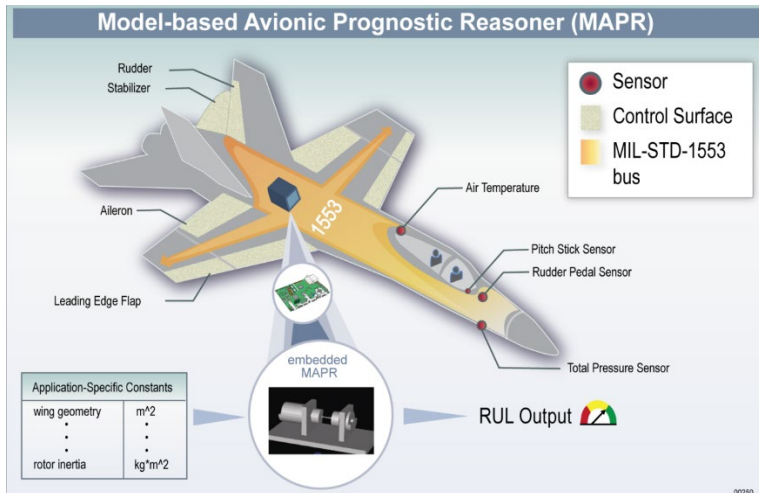


Figure 1: Concept for a Model-based Avionic Prognostic Reasoner (MAPR).

The proposed solution methodology seemed straightforward and not complicated: (1) solve a set of simultaneous equations and (2) use statistical methods, such as principal component analysis (PCA), K-nearest neighbor (KNN), and Euclidean distance methods; and (3) show how the test bed and methods would detect, isolate, and characterize EMA faults. An example of a set of models for multivariate analysis is shown in Figure 2 [5].

DC Motor    Input    Model Creation    Model Estimation    Analysis

You know the value of the Inertia  $J_1$  and  $J_2$ , and rotational damping  $B_1$  and  $B_2$ , or the torsional Spring  $K$ . You can follow the following steps to estimate the values of  $k$ ,  $b_1$  and  $b_2$

- Derive the state-space model for the dynamic system below. Since you know the value of some parameters and the elements of the A matrix are coupled to each other, this model is called partially known state-space model.
- Estimate the partially known state-space model with real measurement.

Derivation of State Space model from original equations:

$$J_1 \dot{x}_1' = -k x_1 - (b_1 + b_{12}) x_1' + k x_2 + b_{12} x_2' + T$$

$$J_2 \dot{x}_2' = -b_2 x_2' + k (x_1 - x_2) + b_{12} (x_1' - x_2')$$

- Re-arrange and collect terms ==>
 
$$J_1 \dot{x}_1' = -k x_1 - (b_1 + b_{12}) x_1' + k x_2 + b_{12} x_2' + T$$

$$J_2 \dot{x}_2' = k x_1 + b_{12} x_1' - k x_2 - (b_2 + b_{12}) x_2'$$
- Normalize ==>
 
$$x_1' = -k/J_1 x_1 - (b_1 + b_{12})/J_1 x_1' + k/J_1 x_2 + b_{12}/J_1 x_2' + T/J_1$$

$$x_2' = k/J_2 x_1 + b_{12}/J_2 x_1' - k/J_2 x_2 - (b_2 + b_{12})/J_2 x_2'$$
- Add additional states ==>
 
$$x_1'' = x_1'$$

$$x_1' = -k/J_1 x_1 - (b_1 + b_{12})/J_1 x_1' + k/J_1 x_2 + b_{12}/J_1 x_2' + T/J_1$$

$$x_2'' = k/J_2 x_1 + b_{12}/J_2 x_1' - k/J_2 x_2 - (b_2 + b_{12})/J_2 x_2'$$
- Write as Matrix-Vector product ==>
 
$$\begin{bmatrix} x_1'' \\ x_1' \\ x_2'' \\ x_2' \end{bmatrix} = \begin{bmatrix} 0 & 1 & 0 & 0 \\ -k/J_1 & -(b_1 + b_{12})/J_1 & k/J_1 & b_{12}/J_1 \\ 0 & 0 & 0 & 1 \\ k/J_2 & b_{12}/J_2 & -k/J_2 & -(b_2 + b_{12})/J_2 \end{bmatrix} \begin{bmatrix} x_1 \\ x_1' \\ x_2 \\ x_2' \end{bmatrix} + \begin{bmatrix} 0 \\ T/J_1 \\ 0 \\ 0 \end{bmatrix}$$
- Add Output equation ==>
 
$$\begin{bmatrix} \text{pos}_A \\ \text{pos}_L \end{bmatrix} = \begin{bmatrix} 1 & 0 & 0 & 0 \\ 0 & 0 & 1 & 0 \end{bmatrix} \begin{bmatrix} x_1 \\ x_1' \\ x_2 \\ x_2' \end{bmatrix} + \begin{bmatrix} 0 \\ 0 \end{bmatrix}$$

Figure 2: Example of Multivariate Analysis Modeling.

The data set was collected from a test bed (see Figure 3) for an EMA comprising a brushless DC motor (BLDC) driven by an H-bridge switching type of commutation (see Figure 4). [5]

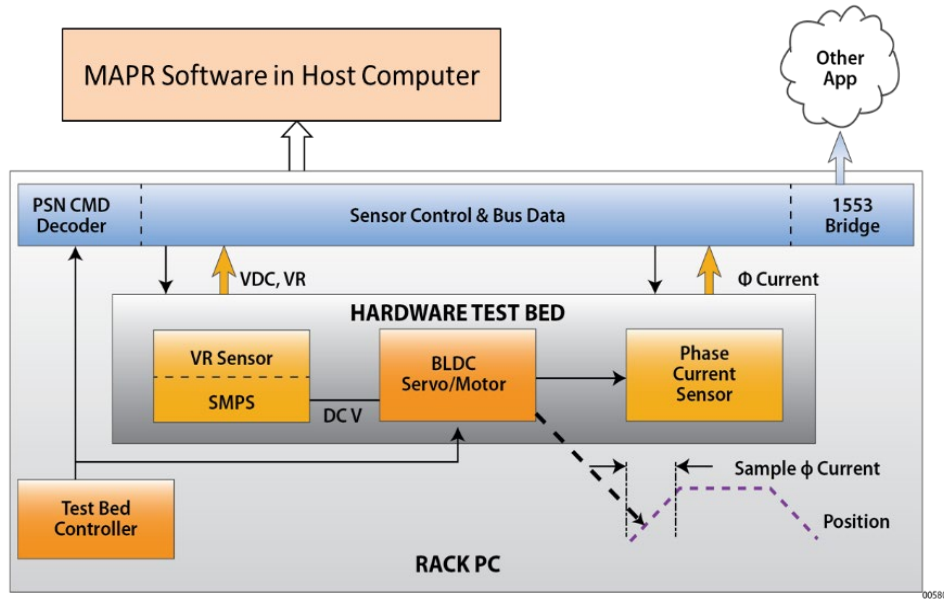


Figure 3: Test Bed Diagram.

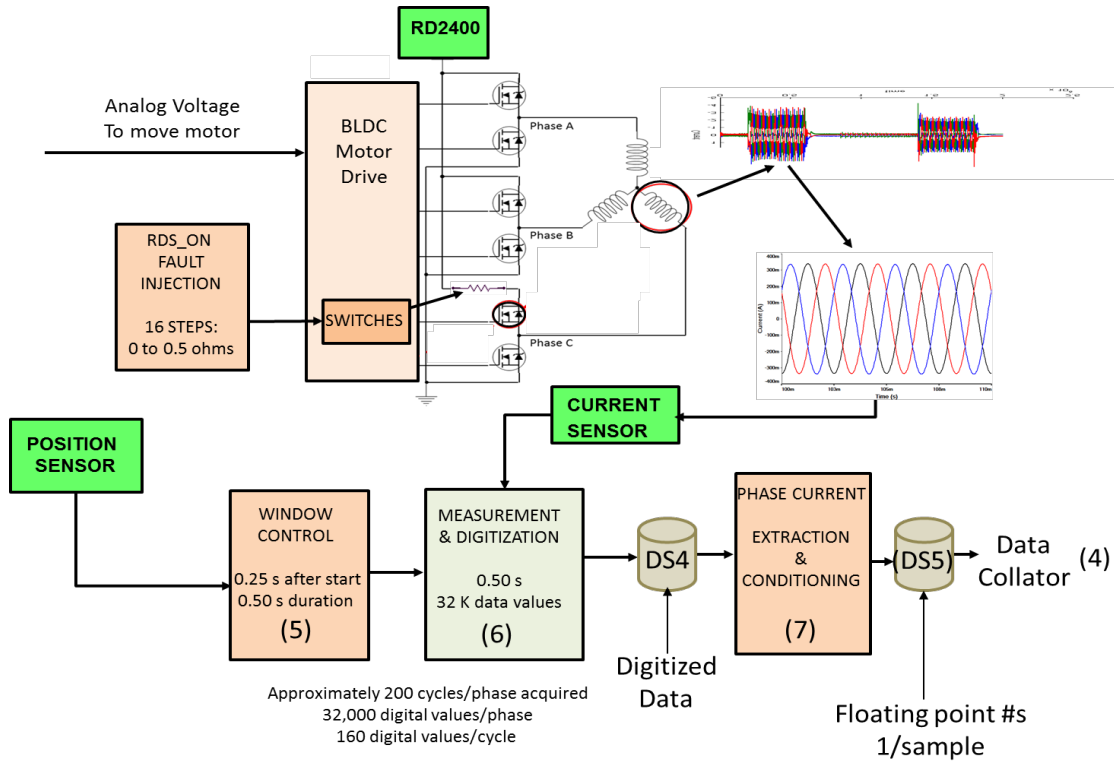


Figure 4: EMA Test Diagram.

In practice, the proposed initial methods were found not feasible because of, for example, the following: (1) analysis methods that produced information suitable for classification rather than diagnosis or prognosis; (2) noisy data (see Figure 5); (3) dependent, rather than independent, data; and (4) difficulty in processing test data to identify, extract, and use leading indicators of failure for prognostic purposes [5].

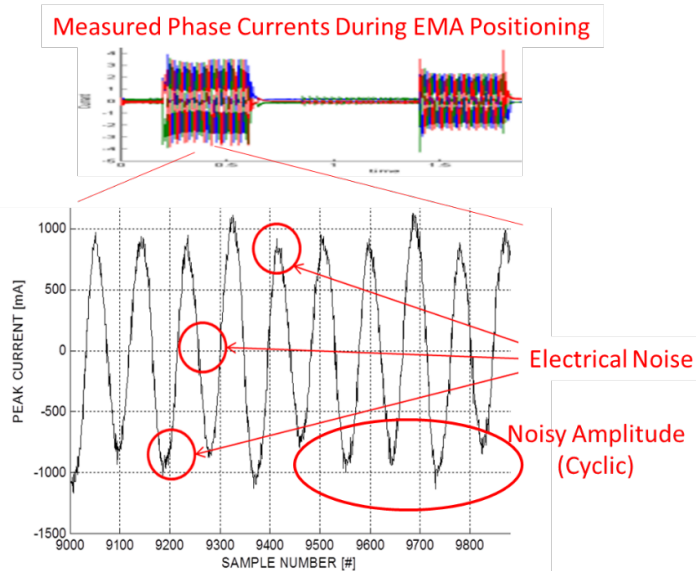


Figure 5: Example of Noisy Phase Current.

A unique root-mean-square (rms) method was created for quantifying measured values of phase currents. A methodology based on KNN and distance methods is used to process feature data extracted from condition-based data (CBD) to unequivocally identify and isolate various types of faults, and to prognose future times of functional failure [5], [6].

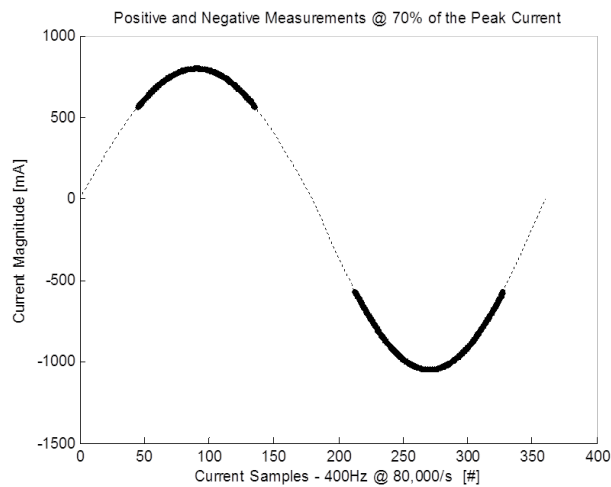


Figure 6: Peak Threshold Values for Calculating RMS.

## 2. MVA SOLUTION: APPROACHES AND RESULTS

### Fault-Classification Algorithm

**PCA-based approach:** An original objective of the program was to develop a fault-classification algorithm based on principal component analysis (PCA) that would model a process, program rules to produce a vector of residual errors (such as the following errors seen in Figure 7), and group those errors using machine-learning methods such as support vector machines (SVM) and a self-organizing map (SOM) to determine the best approach for fault-classification solutions in complex EMA systems [5].

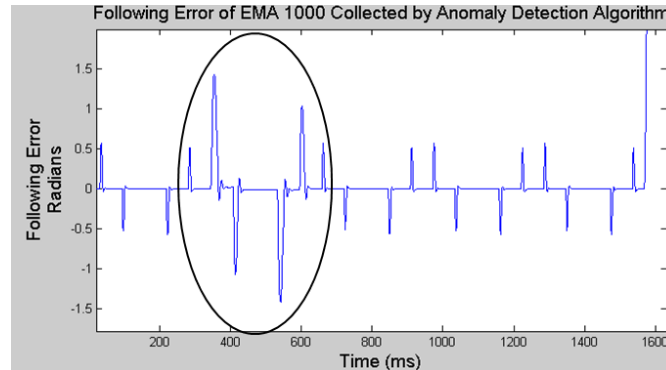


Figure 7: EMA Anomaly, Following Error Due to a Degraded Transistor in an H-bridge.

Clustering algorithms such as K-Means, Jarvis-Patrick, or Unsupervised k-Windows for fault classification were to be considered to categorize excursions. Algorithms of this type are used to group the incoming data into separate clusters based on their statistical behavior.

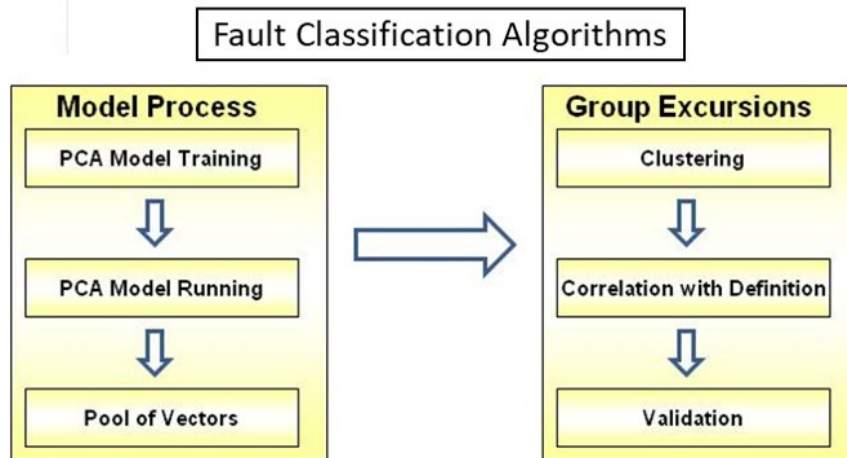


Figure 8: Block Diagram for Using PCA to Cluster Errors.

The main objective of clustering is to find similarities between events and then group similar data or events together to assist in understanding relationships or classifications that might exist among them. [7]-[9] Also, self-organizing maps (SOM), support vector machines (SVM), and Bayesian classification were researched to classify them as either feed analyzer or effluent analyzer faults, while PCA is used to model processes by providing information about the state of the process. Those methodologies will be

categorized for different applications, and the strengths and weaknesses will be summarized and documented.

**Result:** We concluded that using a PCA-based approach to develop fault-classification algorithms for EMAs had unnecessary redundancy. The rationale for that conclusion included the following:

- PCA is a statistical procedure to convert a set of observations of possibly correlated variables into a set of uncorrelated variables (principal components). Given a EMA as a base platform, given an EMA test bed, given designed, known faults that are injected into the test bed,
- The set of principal components is known and is constrained by the specific EMA used in the test bed, the selection of the nodes at which faults are to be injected, the type of fault injected into the test bed, and the sensors (data collector) types and locations used in the test bed.

PCA and classification is useful when historical data exist and data relationships are uncertain, when it is unclear how many uncorrelated variables are in the data; and when it is not known how to group uncorrelated variables.

### **MVA Solutions: Modeling and Data Processing**

A common MVA-solution approach for identifying and isolating a number of faults, N, is to set up and solve a set of N simultaneous equations. For example, let FD represent a feature data associated with three phase currents (A, B, & C) and the number of faults be limited to three, then basic MVA modeling yields

$$FD_A = FD_{A1} + FD_{A2} + FD_{A3} \quad (1)$$

$$FD_B = FD_{B1} + FD_{B2} + FD_{B3} \quad (2)$$

$$FD_C = FD_{C1} + FD_{C2} + FD_{C3} \quad (3)$$

Then let V represent the phase voltage,  $Z_W$  represent the impedance of the EMA-motor stator winding,  $Z_T$  represent the total impedance of the switching transistor and the connections to-from the EMA-motor stator winding, and  $-Z_M$  represent the effective impedance of the EMA-motor load reflected back into the EMA-motor stator winding. EQ. (1) through (3) become

$$FD_A = V_A(1/(Z_{WA} + Z_{TA} - Z_{MA})) \quad (4)$$

$$FD_B = V_B(1/(Z_{WB} + Z_{TB} - Z_{MB})) \quad (5)$$

$$FD_C = V_C(1/(Z_{WC} + Z_{TC} - Z_{MC})) \quad (6)$$

where  $V_A$ ,  $V_B$ , and  $V_C$  are of the form

$$V = V_{DC} + V_{AC}(\cos(\omega t + \theta) + V_{NOISE}) \quad (7)$$

With the restriction that the magnitude of  $-Z_M$  be identical for all measured phase currents and  $V$  be identical for all measured phase currents, it was felt that using KNN and distance methods, any fault in any stator winding or switching-transistor circuit or excessive loading could be detected and isolated.

### 3. MVA AND NOISE

#### MVA Solutions: Noise is an Issue

Statistical-based MVA modeling is difficult to apply in practice, including test beds because of noise issues. CBD (sampled by sensors and processed by hardware, firmware, and software) contains both FD and noise. Here, noise is defined as anything not related to FD,

$$CBD = FD + Noise \quad \text{model for noisy CBD} \quad (8)$$

**Power-supply noise:** The DC voltage from a power-supply input to an EMA is noisy: the most significant in amplitude being the damped-ringing responses due to abrupt changes in load (see Figure 9).

**Actuator-movement noise:** The magnitude of measured phase currents varies. One type of variation (noise) is associated with whether the actuator is lifting a load, such as wing surface, or lowering a load. Referring to Figure 8, the magnitude of the phase current is larger when a load is lifted compared to when a load is lowered.

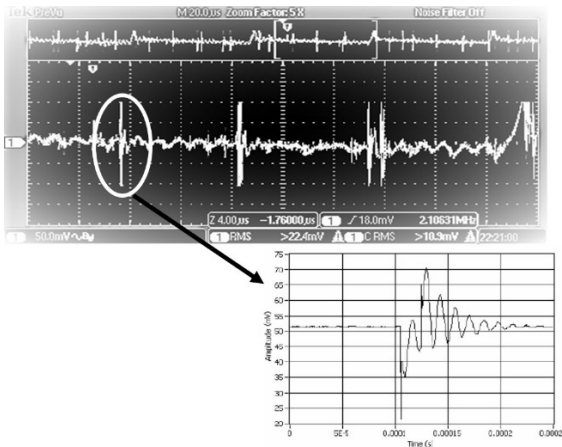


Figure 9: EMA Input Voltage – from the RD2400 (Green) Seen in Figure 4.

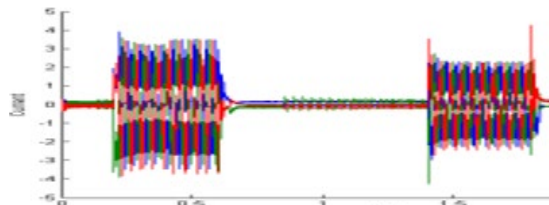


Figure 10: Phase Currents – Lifting (Left) and Lowering (Right) a Load.

**Inertia and momentum noise:** Move up (lift) or down (lower) commands cause an EMA to encounter load inertia and, similarly, when an actuator stops lifting or lowering a load, it encounters load momentum, which results in another type noise (Figure 11).

**Normal-load and excessive-load noise:** There is noise associated with the weight of a load - a normal load or an excessive load. For example, the right-hand plot in Figure 12 exhibits more harmonic distortion compared to the left-hand plot.

**Electrical and cyclic-amplitude noise:** Referring back to the bottom plot in Figure 5, phase current data exhibits noise marked ‘Electrical Noise’ and ‘Noisy Amplitude’ - electrical noise is primarily due to switching noise in the input DC voltage and noisy amplitude is due to level shifting because the three stator windings have a floating, common reference (refer back to Figure 4).

### Noise Filtering and Mitigation Methods

**Sampling and accuracy:** A common method for filtering out noise is use data sampling as a low-pass filtering method: but at what sampling frequency? Since the frequency of the phase current is about 400 Hz, it might seem logical to sample at 800 Hz – to satisfy the Nyquist criteria: but that turns out to be too low of a sampling frequency.

For example, suppose you want to measure the AC component of FD with an accuracy of at least 90%: then from EQ. (8) and letting  $S$  represent sampling frequency,  $N$  represent noise, and  $\alpha$  represent accuracy (as a ratio),

$$S \geq (2/\alpha)N_{FREQUENCY} \tag{9}$$

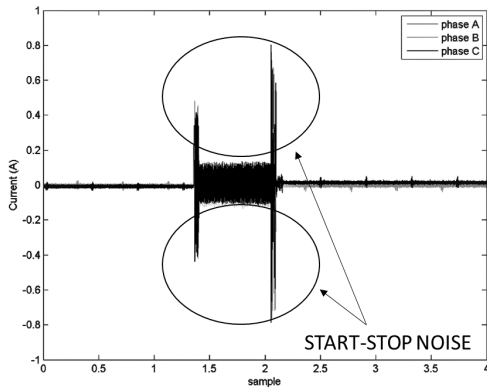


Figure 11: Noise Associated with the Start-Stop Lifting of a Load.

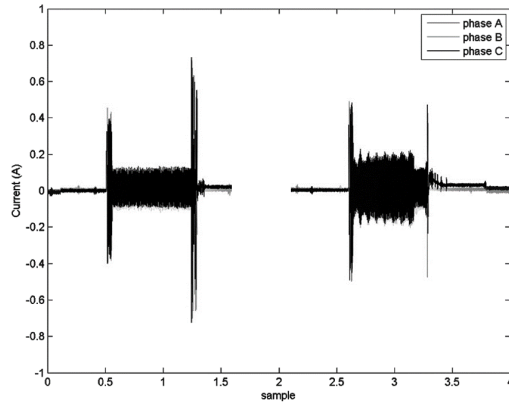


Figure 12: Normal Load (Left), Excessive Load (Right).

For a frequency of 400 Hz, EQ. (9) results in,

$$S \geq (2/0.10)400 = 8 \text{ kHz}$$

It turns out that 8 kHz is also too low because the frequency of the switching noise seen in Figure 9 is a little over 2.5 kHz, and from EQ. (9), you need a sampling frequency of more than 50 kHz to satisfy a 10% accuracy requirement.

**Sampled data and loading:** Since an objective of SBIR program is to detect excessive loading, such as too much weight and/or excessive friction, you need to sample data when the EMA is lifting a load rather than lowering a load. This means you need to provide a method for detecting the start of a positioning command and you need to determine whether the positioning direction is up or down. The test bed needs a positioning sensor, as shown by a green-colored block in Figure 4, and it needs firmware (or software) programming logic to setup a sampling window

**Sampling Window:** Evaluation of the right-side plot in Figure 12 and experimenting with EMA positioning commands leads the following window specifications (block 5 in Figure 4): (1) start sampling 0.25 s after a move-up command, (2) sample at 64 kHz for 0.50 s (32,000 data samples).

### MVA Solutions: Fault Testing

**Winding and Load Faults:** The execution of a design of experiment when a winding type of fault (a reduced impedance in a stator winding) or a loading type of fault (increased lifting weight) is injected into the test bed yields results as predicted by the models of EQ. (4) – EQ. (6): referring to Figure 13, when a winding fault is injected into the test bed, only one of the three phase currents increase in amplitude, and when a load/friction fault is injected into the test bed, all three phase currents increase in amplitude.

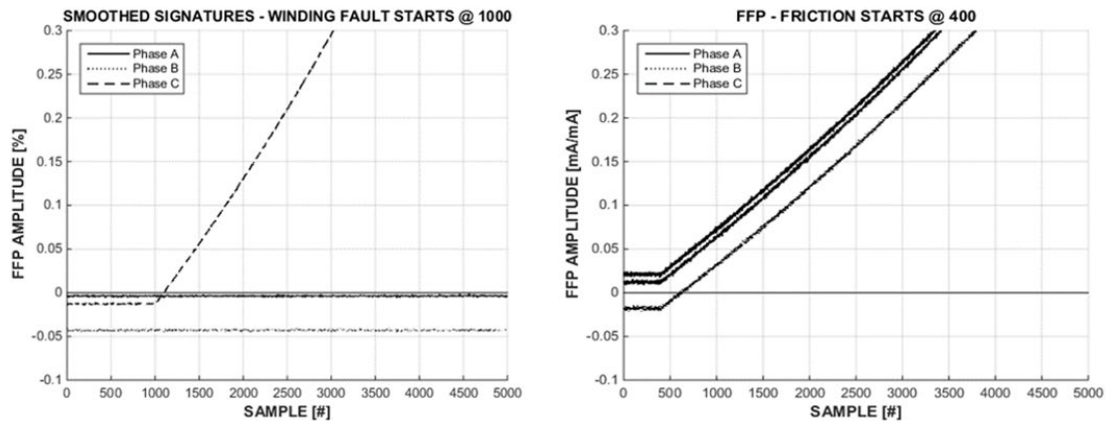


Figure 13: Phase Currents for a Winding Fault (Left) and Load (Friction) Fault (Right).

**Switching Transistor Fault:** A switching transistor fault is injected into the test bed by inserting a low-value resistance in series with one of the six transistors in the h-bridge. The experiment is deemed a failure because there is no significant in measured amplitude of the phase currents. This is because the on-resistance of a switching transistor, compared to the impedance of a stator winding, is too low: this is verified by experimentation and simulation. A degraded transistor in one of the six current branches in the h-bridge (Figure 4) causes a change in the current amplitude of either the positive or the negative half of one of the three phase currents. Because of a floating reference topology in the motor of the EMA (right-hand diagram in Figure 14), the reference levels of the three phase currents shift with respect to each other (left-hand plot in Figure 14).

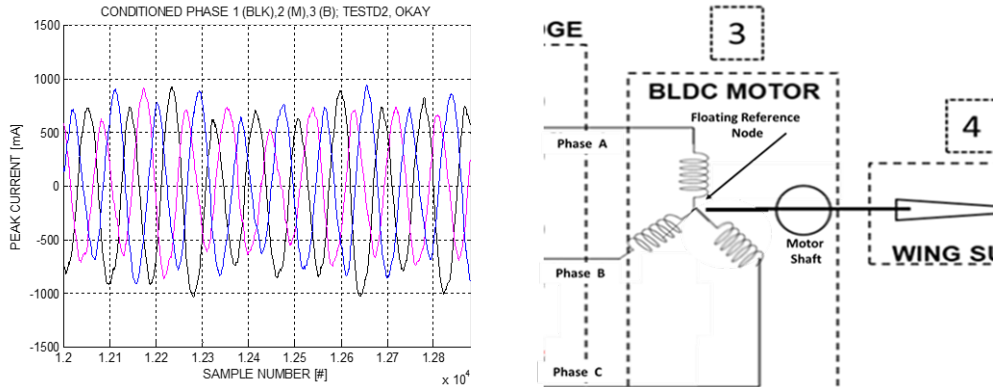


Figure 14: Data Caused by a Degraded Transistor (left) and BLDC Motor (Right).

More importantly, the impedance presented by those switching transistors is significantly smaller in comparison to the impedance of the stator windings: changes in the amplitude caused by transistor degradation are lost in the noise of all other variations in current amplitude. Even when the series impedance of a rectifying branch in the h-bridge is increased from  $0.01 \Omega$  to  $1.0 \Omega$  (a functionally-failed value), the maximum change in peak current was about 25 mA – less than 3.0% (see Figure 15).

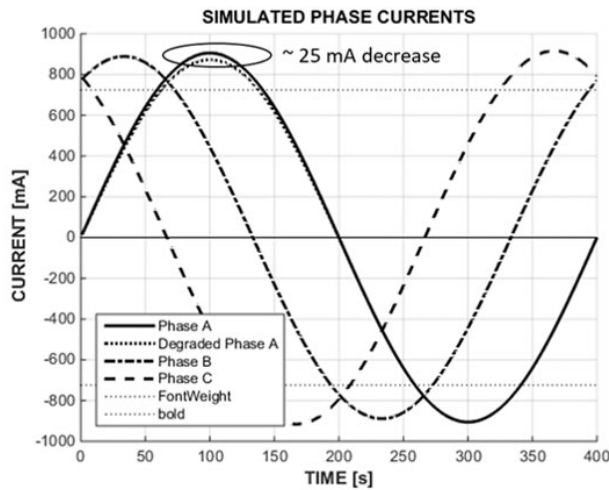


Figure 15: Amplitude Change – Transistor On-Resistance Increased by 10x.

#### 4. MVA SOLUTION: SPECIAL RMS

We developed a unique, innovative solution: (1) define peak-threshold levels ( $T_{PEAK}$ ); (2) truncate all values of current below the positive threshold and above the negative threshold; (3) calculate the magnitudes of the positive phases ( $P_{RMS}$ ) and negative phases ( $N_{RMS}$ ) and (4) sum the magnitudes. This method emphasizes any differences between peak current values and the defined thresholds.

##### Algorithm: Special RMS,

$$T_{PEAK} = 0.70 \quad \text{set threshold level} \quad (10)$$

$$I_{PEAK} = 900 \quad \text{set nominal value of peak current (mA)} \quad (11)$$

$$I_{TRUNC} = T_{PEAK} * I_{PEAK} \tag{12}$$

When  $(\square(\square) > 0) \ \&\& \ (\square(\square) > \square_{\square\square\square\square\square})$  then letting  $P = \text{count of true}$

$$P_{RMS} = [(1/P) \sum_1^n (I(n) - I_{TRUNC})] \quad \text{do not square} \tag{13}$$

When  $(\square(\square) < 0 \ \&\& \ \square(\square) < -\square_{\square\square\square\square\square})$  then letting  $N = \text{count of true}$

$$N_{RMS} = [(1/N) \sum_1^n (I_{TRUNC} - I(n))] \quad \text{do not square} \tag{14}$$

Take a difference summation

$$I_{RMS} = P_{RMS} + N_{RMS} \quad \text{Sum the differences} \tag{15}$$

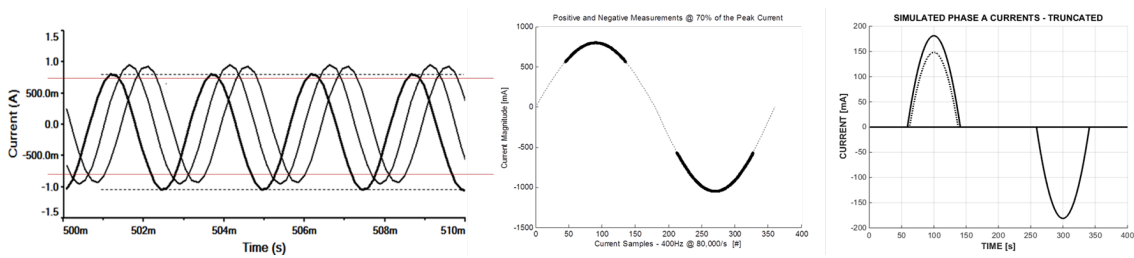


Figure 16. Illustration of Special-rms Method

### Algorithm Result: Examples

The left-hand plot in Figure 17 illustrates the result of applying the special-rms algorithm to one sinusoid of a phase current in which the switching transistor in the positive branch is degraded. The algorithm was applied to all three sets of measured current data and plotted as shown in Figure 17.

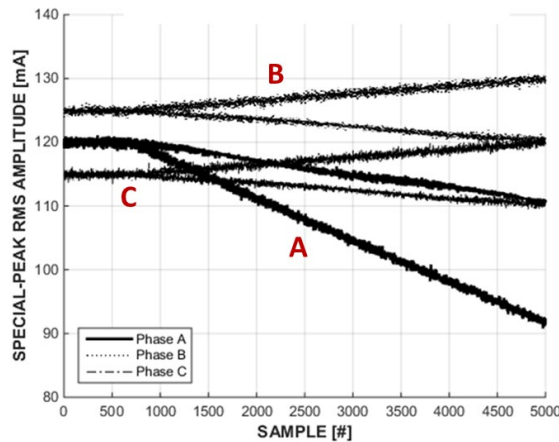


Figure 17: Plots of Test Data (3 Phases) After Special-rms Method.

The data is collected and conditioned, transformed to functional-failure signature (FFS) data, further conditioned, and input to a prediction algorithm: one data point at time, to produce (1) the conditioned data shown in Figure 18 (left) ; (2) the conditioned FFS data

shown in Figure 18 (right); and prognostic information from the prediction algorithm is plotted in Figure 19.

### Prognostic Information

The prediction algorithm accepts FFS input data, processes the input, and produces prognostic information – one data point at a time. The prognostic information comprises Remaining Useful Life (RUL), prognostic horizon (PH), and State of Health (SoH). The FFS data plotted in Figure 18 produced the prognostic information plotted in Figure 19.

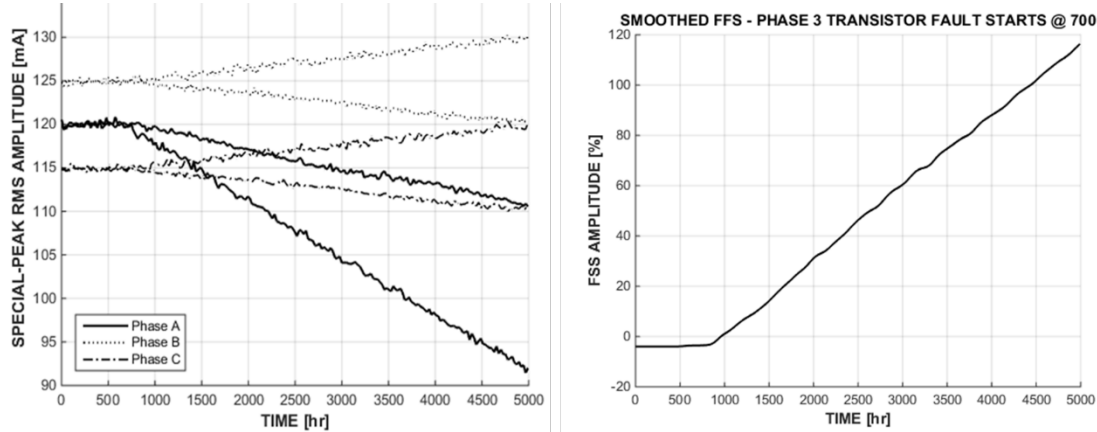


Figure 18: Conditioned Data (Left) – Transformed to Smoothed FFS (Right).

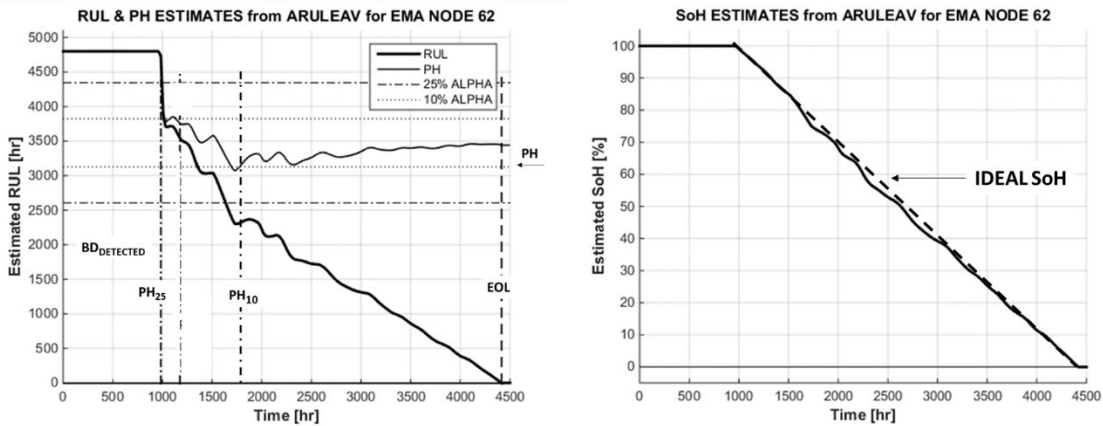


Figure 19: Prognostic Information – RUL & PH (Left) and SoH (Right).

### Prognostic Accuracy

The prediction algorithms in a program called ARULEAV (Adaptive RUL Estimation – Advanced Version) employs a number of algorithms to produce very accurate prognostic estimates (refer to Figure 20):

Treat data point as a particle having momentum and inertia that tend to maintain direction and speed – use weighting and coefficients.

Data points tend to move in a data space from lower-left corner to upper-right corner – a random walk.

Data points form a characteristic curve that is represented by three data spaces concatenated together from bottom to top, left to right, at the corners – employ piece-wise solution methods.

Employ Kalman-like filtering

- Remember the time when degradation is detected (BD)
- Remember the last data point
- Use the data space models to predict where the next data point should be
- Compare predicted point to sampled next data point – the sample time (ST)
  - Compute a compromise between predicted and actual data point
  - Adjust the model lengths to correspond to the computed point
  - Use the adjusted model to estimate when functional failure (EOL) occurs
  - Compute  $RUL = EOL - ST$
  - Compute  $SoH = 100\% * (EOL - RUL) / EOL$
  - Compute  $PH = ST + RUL = \text{estimated EOL (relative to BD)}$

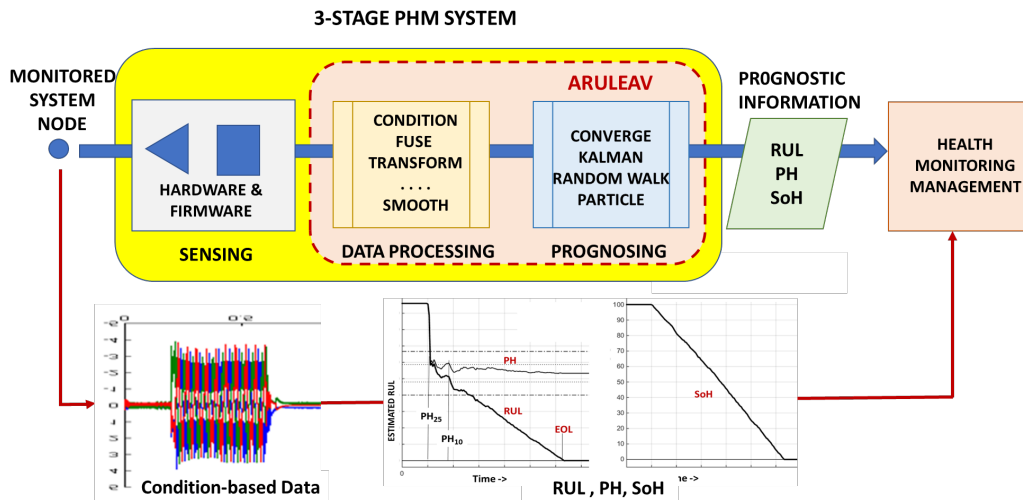


Figure 20. Diagram of a 3-stage PHM System.

ARULEAV also incorporates fast-convergence algorithms that generally produces PH estimates within an alpha ( $\alpha$ ) accuracy of 25% within 10 data points with a standard deviation of 3 points.

## 5. CONCLUSION

Statistical modeling and methods such as PCA and machine learning methods such as SVM and Euclidean distance proved not be helpful in prognostic enabling an EMA: primarily because we designed and built an EMA test bed with predetermined fault injection locations and means, and data was collected using known sensors located at specific nodes in the test bed. Therefore, the existence of or lack of correlation between the variables of the collected data was known, and the principal components of the data (voltage, ripple, phase current, and so on) was known or readily identified by examination of the data.

We did use the concepts of KNN and distance methods to identify and located faults: winding versus load/friction versus switching transistor.

The filtering and mitigation of noise was the most significant issue that had to be addressed to provide a prognostic solution for winding and load faults in an EMA. Because of the large difference in the values of the impedance of the EMA stator windings compared to the on resistance of switching transistors, a special-rms method had to be developed to detect and process phase currents.

In the end, we developed an effective solution for EMA monitoring. The prognostic information is produced by conditioning and transforming phase current data into signature data as input to prediction algorithms resulted in fast and accurate prognostic information.

## References

- [1] Kunst, et al., (2008) “Electronic Prognostics Solutions for Electromechanical Actuator Systems”, IEEE PHM Conference, Denver, CO, October 2008
- [2] Kunst, et al., (2009) “Damage Propagation Analysis Methodology for Electromechanical Actuator Prognostics”, IEEE Aerospace Conference, Big Sky, MT, March 2009
- [3] M. Walker, R. Kapadia, B. Sammulu, and M. Venkatesh. (2007) “A Model-based Reasoning Framework for Condition-based Maintenance and Distance Support”. Automation and Controls Symposium, ASNE, Biloxi, MS. December 2007.
- [4] R. Kapadia, G. Stanley, and M. Walker. (2007) “Real World Model-based Fault Management”. Proc. of the 18th International Workshop on Principles of Diagnosis, Nashville, TN. May 2007.
- [5] NASA Phase 2 Proposal A1 12-9941, (2012) “Physical Modeling for Anomaly Diagnostics and Prognostics,” Ridgetop Group, Inc., 24 November 2012.
- [6] Goodman, Douglas L.; Hofmeister, James P.; and Szidarovszky, Ferenc; 2019 (Pending), *Prognostics and Health Management: A Practical Approach Using Conditioned-Based Data*, 1<sup>st</sup> Edition, John Wiley & Sons, Ltd, The Atrium, Southern Gate, Chichester, West Sussex, PO19 8SQ, United Kingdom, ISBN: 9781119356653, 2019, pp. 255-274, 300-311.
- [7] Ding, C., & He, X., (2004) “K-means clustering via principal component analysis,” Proceedings of the 21st International Conference on Machine Learning, 2004
- [8] A. Vathy-Fogarassy, A. Kiss, J. Abonyi, (2007) “Improvement of Jarvis-Patrick. Clustering Based on Fuzzy Similarity,” Lecture Notes in Computer Science, 2007
- [9] M. N. Vrahatis, B. Boutsinas, P. Alevizos, and G. Pavlides (2002) “The new k-windows algorithm for improving the k-means clustering algorithm,” Journal of Complexity, 18:375–391, 2002

## Bibliography

- [1] Hofmeister, J., Wagoner, R. and Goodman, D. (2013) “Prognostic Health Management (PHM) of Electrical Systems using Conditioned-based Data for Anomaly and Prognostic Reasoning,” Chemical Engineering Transactions, Vol. 33, pp. 992-996.
- [2] Kumar, S. and Pecht, M. (2010) “Modeling Approaches for Prognostics and Health Management of Electronics,” *International Journal of Performability Engineering*, Vol. 6, No. 5, pp. 467-476.

- [3] Pecht, M. (2008) *Prognostics and Health Management of Electronics*. Hoboken, NJ: John Wiley & Sons.
- [4] O'Connor, P. and Kleyner, A. (2012) *Practical Reliability Engineering*. Chichester, UK: John Wiley & Sons.
- [5] Hofmeister, James P.; Goodman, Douglas, L.; and Szidarovszky, Ferenc (2018); "Transforming Condition-based Data Signatures into Functional Failure Signatures," IEEE 2018 Aerospace Conference, Big Sky, MT, 3-9 March, 2018.
- [6] Saxena, A., Celaya, J., Saha, B., Saha, S. and Goebel, K. (2009) "On Applying the Prognostic Performance Metrics," Annual Conference of the Prognostics and Health Management Society (PHM09), San Diego, CA, 27 Sep.-1 Oct. 2009.